Journal of Neuroscience Research 85:139–152 (2007)

Mitochondrial Isocitrate Dehydrogenase Protects Human Neuroblastoma SH-SY5Y Cells Against Oxidative Stress

Sun J. Kim,[1,5] Tae Y. Yune,[5] Ching T. Han,[1] Young C. Kim,[2] Young J. Oh,[3] George J. Markelonis,[4] and Tae H. Oh[5]★

[1]Sogang University, College of Science, Department of Life Science, Seoul, Korea
[2]Seoul National University, College of Pharmacy Seoul National University, Seoul, Korea
[3]Yonsei University, College of Science, Department of Biology, Seoul, Korea
[4]University of Maryland School of Medicine, Department of Anatomy and Neurobiology, Baltimore, Maryland
[5]Kyung Hee University, Aging and Brain Diseases Research Center, Seoul, Korea

The neuroprotective effect of mitochondrial isocitrate dehydrogenase (IDPm), an enzyme involved in the reduction of $NADP^+$ to NADPH and the supply of glutathione (GSH) in mitochondria, was examined using SH-SY5Y cells overexpressing IDPm (S1). S1 cells showed higher NADPH and GSH levels than vector transfectant (V) cells and were more resistant to staurosporine-induced cell death than controls. Staurosporine-induced cytochrome c release, caspase-3 activation, and production of reactive oxygen species (ROS) were significantly attenuated in S1 cells as compared to V cells and reduced by antioxidants, trolox and GSH-ethyl ester (GSH-EE). Staurosporine-induced the release of Mcl-1 from mitochondria that formed a complex with Bim. Mcl-1 was then cleaved to a shortened form in a caspase-3 dependent manner; its release was attenuated far more in S1 than in V cells after staurosporine treatment. Finally, the staurosporine-induced decrease in mitochondrial membrane potential ($\Delta\psi_m$) was correlated with the time of mitochondrial Mcl-1 release; the loss of $\Delta\psi_m$ was attenuated significantly in S1 cells as compared to that in V cells. These results suggest that the neuroprotective effect of IDPm may result from increases in NADPH and GSH levels in the mitochondria. This, in turn, inhibits mitochondrial ROS production after cytochrome c release, which seems to be mediated through Mcl-1 release.

Key words: cytochrome c; GSH; Mcl-1; NADPH; staurosporin

Glutathione (GSH) depletion resulting from oxidative stress contributes to neuronal cell death and pathologic processes in neurodegenerative diseases including Parkinson's disease (PD) and Alzheimer's disease (AD) as well as normal aging (Sian et al., 1994; Bains and Shaw, 1997; Schulz et al., 2000; Woltjer et al., 2005). An early and highly selective decrease in GSH in the substantia nigra is present in PD (Sofic et al., 1992); low levels of GSH lead to the degeneration of cultured dopaminergic neurons (Canals et al., 2003; Hsu et al., 2005). After brain focal ischemia in rats, cell death and the degree of infarction is closely associated with the degree of mitochondrial glutathione loss throughout the brain region affected (Anderson and Sims, 2002). In a related manner, it was reported that GSH protects neurons from the toxicity of 6-hydroxydopamine (6-OHDA) and 1-methyl-4-phenylpyridinium ion (MPP^+) and from apoptosis induced by dopamine (Spina et al., 1992; Gabby et al., 1996).

GSH is a well-known antioxidant usually present as the most abundant, low-molecular-mass thiol in most organisms; it plays an important role in cells by removing oxidants formed in cells under steady state or oxidative environments (Griffith and Meister, 1985). GSH helps maintain cysteinyl-thiol ($R\text{-}CH_2\text{-}SH$) groups of proteins in a reduced state; this is often necessary for their functional integrity (Inoue, 1989). In mitochondria, superoxide anions produced intrinsically by leakage of electrons during uncoupled aerobic respiration are reduced rapidly to H_2O_2 by manganese superoxide dismutase. GSH, in tandem with the enzymes GSH peroxidase and GSSG reductase, serves to detoxify H_2O_2 to water and molecular oxygen. Furthermore, mitochondrial GSH peroxidase might contribute to metabolizing H_2O_2 because catalase, which metabolizes H_2O_2, is absent in the mitochondria of most animal cells

Sun J. Kim and Tae Y. Yune contributed equally to this article.

Contract grant sponsor: MOST Neurobiology Research Program, Seoul City Research Fund, Post Bk 21 Program and Brain Research Center of the 21st Century Frontier Research Program (Korea).

★Correspondence to: Tae H. Oh, PhD, Aging and Brain Diseases Research Center, Medical Building, Kyung Hee University, Dongdaemun-gu, Hoegi-dong 1, Seoul, 130-701, Republic of Korea.
E-mail: toh@khu.ac.kr

Received 5 June 2006; Revised 7 August 2006; Accepted 5 September 2006

Published online 30 October 2006 in Wiley InterScience (www.interscience.wiley.com). DOI: 10.1002/jnr.21106

(Esworthy et al., 1997). Therefore, the reduced GSH required for the activity of mitochondrial GSH peroxidase, remains as a defense for metabolizing H_2O_2 through GSH redox. In this regard, glutathione should be reduced to GSH by glutathione reductase, which uses the reducing potential of NADPH. A recent report shows that the NADPH required for the production of GSH in the mitochondria is produced by mitochondrial isocitrate dehydrogenase (IDPm) (Jo et al., 2001), whereas the NADPH is generated by the pentose phosphate pathway in the cytoplasm (Gaetani et al., 1989).

The isocitrate dehydrogenases (ICDHs) catalyze oxidative decarboxylation of isocitrate into α-ketoglutarate and require either NAD^+ or $NADP^+$ as coenzyme yielding NADH and NADPH, respectively. NADPH is an essential reducing equivalent for the regeneration of GSH by glutathione reductase and for the activity of the NADPH-dependent thioredoxin system (Deneke and Fanburg, 1989). In mammals, three classes of ICDH isoenzymes exist: mitochondrial NAD^+-dependent ICDH, mitochondrial $NADP^+$-dependent ICDH (IDPm), and cytosolic $NADP^+$-dependent ICDH (Plaut and Gabriel, 1983). The IDPm gene was cloned recently and the authors suggested that it might provide NADPH as an electron donor for GSH regeneration in mitochondria (Jo et al., 2001). In this regard, increased mitochondrial GSH, possibly provided by IDPm, has exhibited a protective function against H_2O_2-mediated apoptosis in mouse fibroblast NIH3T3 cells (Jo et al., 2001).

The functional role of IDPm has not been examined in the nervous system. We investigated the role of IDPm in staurosporine-induced cell death in the SH-SY5Y, human neuroblastoma cell line. For this study, IDPm was overexpressed in SH-SY5Y cells, and we examined its neuroprotective effect and signaling mechanisms. Our results showed that cells overexpressing IDPm were more resistant to staurosporine-induced oxidative stress by inhibiting mitochondrial production of ROS after cytochrome c release. Furthermore, we found that mitochondrial cytochrome c release seemed to be mediated by Mcl-1, which formed a complex with Bim and was released from mitochondria after staurosporine treatment.

MATERIALS AND METHODS

Materials

Materials for cell culture were obtained from Gibco (Rockville, MD). All other chemicals such as 3-[4,5-dimethylthiazol- 2-yl]-2,5-diphenyl tetrazolium bromide (MTT), staurosporin, nicotinamide, NADPH, GSH, and trypan blue were purchased from Sigma (St. Louis, MO) unless specified.

Cell Culture and Construction of Recombinant Cell Lines

Human neuroblastoma cell line, SH-SY5Y cells were grown in Dulbecco's modified Eagle's medium (DMEM) supplemented with 100 U/ml penicillin, 100 μg/ml streptomycin and 10% (v/v) fetal bovine serum (FBS) at 37°C in a humidified atmosphere under 5% CO_2. The recombinant plasmids containing mouse IDPm cDNA (1,679 bp) ligated into an LNCX-retroviral vector (from Dr. Huh at Kyungbook National University, Korea) or control LNCX-vector plasmids were transfected into SH-SY5Y cells (1×10^7 cells/100 mm dish) using Lipofectamine 2000 (Gibco) according to the manufacturer's protocol. Two days later, cells were transferred to 100-mm dishes in DMEM with 10% FBS and 0.5 mg/ml of G418 (Gibco). After several weeks, individual clones were lifted and tested for expression of the transgene.

Cellular Fractionation of Mitochondrial and Cytosolic Components

After drug treatment, cells (1×10^7 cells/100 mm dish) were washed with PBS, and MS buffer (225 mM mannitol, 25 mM sucrose, 10 mM HEPES, 1 mM EDTA, pH 7.4, 1 μg/ml pepstatin, 2.5 μg/ml leupeptin, 2 μg/ml aprotinin, and 1 mM PMSF) was added directly to the dishes. Cells were harvested by scraping with a rubber policeman and homogenized with a Dounce homogenizer. Cell homogenates were centrifuged at 250 × *g* for 10 min at 4°C to remove the unbroken cells and nuclear particles, and the supernatants were further centrifuged at 8,500 × *g* for 20 min (mitochondrial pellets). After transfer to a new tube, the supernatant was further centrifuged at 100,000 × *g* for 1 hr at 4°C and used as the cytoplasmic fraction (S-100). Depending on subsequent experiments, pellets were resuspended in different solutions or in a lysis buffer A (20 mM Tris-HCl, pH 8.0, 137 mM NaCl, 0.5 mM EDTA, 10% glycerol, 10 mM $Na_2P_2O_7$, 10 mM NaF, 1 mM Na_3VO_4, 1% NP-40, 1 μg/ml aprotinin, 10 μg/ml leupeptin, and 1 mM PMSF). For whole cell extraction, lysis buffer A was added directly to the culture plate and harvested. Protein concentration was determined using the Bradford assay (Bio-Rad, Hercules, CA) or a Micro-BCA assay kit (Pierce, Rockford, IL).

Measurement of IDPm Enzyme Activity, NADPH, and GSH

IDPm enzyme activity was determined by the method of Jo et al. (2001). Mitochondrial pellets were resuspended in PBS containing 0.1% Triton X-100, disrupted by sonication at 40% of the maximum setting with 1 sec interval for 10 sec, and centrifuged at 15,000 × *g* for 30 min at 4°C. The supernatants were used to measure mitochondrial IDPm enzyme activity. IDPm activity was measured by the production of NADPH at 340 nm at 25°C using a Versamax microplate reader (Molecular Devices Corp., Sunnyvale, CA). One unit of IDPm activity was defined as the amount of enzyme catalyzing the production of 1 μmol of NADPH/min. NADPH was determined by the method of Bhamre et al. (2000). Cells were washed in ice-cold PBS, and harvested by immediately adding 0.1 ml of 0.1 N NaOH. After boiling, cell lysates were neutralized to pH 8.0 with Tris/EDTA, and stabilized with 10 mM nicotinamide. Aliquots of each cell lysate (20 ul) were assayed in triplicate in a microplate spectrophotometer according to the cycling procedure described by Wagner and Scott (1994). NADPH and $NADP^+$ standards were used in

the range of 0.0024–0.012 nmol. NADPH was expressed as pmol of NADPH per mg of protein. The GSH level was analyzed by using a GSH assay kit (Calbiochem, San Diego, CA) according to the manufacturer's instructions.

Measurement of Cell Viability

Cytotoxicity induced by staurosporin was determined by trypan blue exclusion and lactate dehydrogenase (LDH) assay (Krohn et al., 1998; Nomura et al., 1999). For trypan blue exclusion and LDH assay, cells (1×10^5) were seeded in 24-well plates. After staurosporin treatment, cells were harvested after trypsinization, and washed with PBS. After centrifugation at $250 \times g$ for 5 min, the pellets were resuspended and incubated in DMEM with 0.1% trypan blue for at least 5 min. Cells were observed and counted using a hemocytometer. To measure the release of LDH into the media 24 hr after staurosporin treatment, 100 μl of media was used according to the manufacturer's instruction (Sigma).

DNA Fragmentation and DAPI Staining

For DNA fragmentation analyses, cells exposed to staurosporin for 12 hr were lysed with buffer (10 mM Tris-Cl, pH 7.6, 20 mM EDTA, 0.5% Triton X-100, 20 μg/ml RNase) followed by phenol extraction and precipitation by 2 volumes of ethanol as described by Nomura et al. (1999). To analyze the degree of DNA fragmentation, DNA samples were resolved on 2% agarose gel containing ethidium bromide, and visualized and photographed under UV illumination using a Chem Imager 4400 (Alpha Innotech Co., San Leandro, CA). For DAPI staining, cells were grown on glass coverslips coated with poly-d-lysine (50 μg/ml). Twelve hours after staurosporin treatment, cells were fixed at 4°C in fixation buffer (4% paraformaldehyde in PBS, pH 7.4) for 30 min, and then rinsed with PBS. Cells were incubated with 1 μg/ml of DAPI in PBS for 10 min, and rinsed three times in PBS and mounted. Cells were observed, and photographed with an Olympus microscope with software accompanying the Cool SNAP camera (Roper Scientific, Tucson, AZ).

Caspase-3 Activity

Caspase-3 enzyme activity was measured by using a caspase-3 assay kit (Chemicon, Temecula, CA). Twelve hours after staurosporin treatment, cells (1×10^5) were harvested, lysed with a lysis buffer. The homogenate was centrifuged at $25{,}000 \times g$ for 10 min at 4°C. The protein concentration was determined by the Micro-BCA assay method. The cell lysate (50 μg of protein in 50 μl) and reaction buffer (100 μl, 50 mM HEPES, pH 7.5, 100 mM NaCl, 1.0 mM EDTA, 10 mM dithiothreitol, 0.1% CHAPS, 10% glycerol) were added to each well and incubated for 10 min at 37°C before adding the substrate (50 μM zDEVD-AFC). The fluorescence (excitation at 400 nm and emission at 505 nm) was measured for 1 hr using a K2 multi-frequency phase fluorometer (ISS Inc., Champaign, IL). The specific activity was calculated relative to a standard curve using recombinant caspase-3 (Upstate Biotechnology, Lake Placid, NY). Experiments were carried out three times to ensure reproducibility.

RNA Isolation and RT-PCR

Total RNA isolation from cultured cells and cDNA synthesis were carried out as described previously (Lee et al., 2004). A 20 μl PCR reaction contained 2 μl first strand cDNA, 0.6 U AmpliTaq polymerase (Perkin-Elmer), 10 mM Tris-HCl, pH 8.3, 50 mM KCl, 2.5 mM $MgCl_2$, 250 μM dNTP, and 10 pmol of each specific primer. Samples were subjected to 30 cycles of 95°C for 1 min, 55°C for 1 min, and 72°C for 2 min on a thermocycler (Perkin-Elmer). PCR primers used are as follows: for IDPm, 5′-GTGCRCGGACC-TCGCAAGCTTGG-3′ (sense), and 5′-GAGTAGTGTCCA-CCGATATCGGTTG-3′ (antisense). For internal control, β-actin, 5′-ATTTGGCACCACACTTTCTACA-3′ (sense), 5′-TCACGCACGATTTCCCTCTCAG-3′ (antisense). To ensure reproducibility, three independent experiments were carried out.

Immunoprecipitation and Western Blot Analysis

For Western blot, cytoplasmic (50 μg) or mitochondrial proteins (10 μg) were separated by 12–15% SDS-PAGE, and transferred onto nitrocellulose membranes. The membranes were blocked with 5% fat-free skim milk in Tris-buffered saline containing 0.1% Tween (TBS-T) for 1 hr at room temperature, and then incubated overnight at 4°C with primary antibody diluted in blocking solution. After washing, membranes were then processed with HRP-conjugated anti-rabbit or anti-mouse secondary antibodies. Immunoreactive bands were visualized by chemiluminescence using Supersignal (Pierce). Experiments were repeated three times to ensure reproducibility. For immunoprecipitation, mitochondrial protein (300 μg) was used. Before immunoprecipitation, protein samples were incubated with 30 μl of protein G Sepharose (50% slurry; Amersham Bioscience, Piscataway, NJ) for 1 hr at 4°C, and these mixed samples were centrifuged at $12{,}000 \times g$ for 1 min to remove nonspecific binding proteins. The supernatant was incubated with 2 μg of anti-Bad, Bak, Bax, Bid, and Bim antibodies and 30 μl of protein G Sepharose at 4°C overnight. The negative control was prepared with protein G Sepharose without antibody. After incubation, beads were washed five times with 0.5 ml of lysis buffer A before boiling in Laemmli sample buffer. The protein samples were immunoblotted as described in the Western blot analysis. The antibodies used for Western blot and coimmunoprecipitation analyses were: rabbit polyclonal antibodies against Bad, Bak, Bax, Bcl-2, Bid, Bim, cytochrome c, Mcl-1 (Santa Cruz Biotechnology, Santa Cruz, CA; 1:500 dilution), and caspase-9, caspase-3 (Cell Signaling, Beverly, CA; 1:1,000 dilution); mouse monoclonal antibodies against Mcl-1 (Pharmingen, San Jose, CA), β-actin (Sigma, 1:2,000 dilution), and cytochrome oxidase IV (Molecular Probe, Eugene, OR; 1:1,000 dilution).

Measurement of ROS Generation

The production of ROS was measured fluorometrically using dichlorodihydrofluorescein diacetate (DCF-DA) and dihydro rhodamine 123 (DHR) (Molecular Probe). After staurosporin treatment, DCF-DA and DHR (10 μM, final concentration) were added to cells. Cells were then washed three times with pre-warmed Locke's buffer (154 mM NaCl,

5.6 mM KCl, 2.3 mM $CaCl_2$, 1 mM $MgCl_2$, 3.6 mM $NaHCO_3$, 5 mM HEPES, 20 mM glucose, pH 7.4) (Ahlemeyer and Krieglstein, 2000). Fluorescence was quantified using a fluorescence plate reader at 488 nm excitation and 510 nm emission wavelength using a Victor^3 Multilabel Plate Reader (Perkin-Elmer). The results were expressed as arbitrary fluorescence units related to μg protein. Cellular fluorescence was imaged using an Olympus fluorescence microscope with software accompanying the Cool SNAP camera.

Measurement of Mitochondrial Membrane Potential ($\Delta\psi_m$)

The mitochondrial membrane potential ($\Delta\psi_m$) in isolated mitochondria and intact cells was measured using the fluorescent probe rhodamine 123 (Rh123, Molecular Probe) with a slight modification as described previously (Ehrenberg et al., 1988; Tay et al., 2005). Rh123 is a lipophilic cation that accumulates in the negatively-charged mitochondrial membrane driven by a $\Delta\psi_m$, and the changes in membrane potential are determined by changes in total fluorescence intensity. Mitochondria were isolated from control SH-SY5Y cells as described previously in Materials and Methods; isolated mitochondria (1 mg/ml protein) were incubated with 100 nM of staurosporine in MS buffer supplemented with 10 mM succinate. After washing, mitochondria were incubated in MS buffer containing Rh123 (50 nM) for 25 min at 25°C. Mitochondria were centrifuged at 8,000 × *g* for 10 min at 4°C and washed twice with MS buffer to remove unincorporated Rh123. After sonication, fluorescence was measured using a Victor^3 Multilabel Plate Reader (Perkin-Elmer) with excitation at 485 nm and emission at 535 nm. For measuring the change of $\Delta\psi_m$ in intact cell, cells were equilibrated with the Rh123 (10 μM) for 30 min at 37°C before the experiment. Then cells were washed three times with pre-warmed Locke's solution before the addition of staurosporine (100 nM). The changes of $\Delta\psi_m$ during staurosporine treatment were measured using a Victor^3 Multilabel Plate Reader.

Statistical Analysis

Data are presented as mean ± SD values. All data were evaluated for statistical significance using Student's paired *t*-test. In all analyses, a *P*-value of <0.05 was considered statistically significant.

RESULTS

Stable Transfection of IDPm Constructs

To investigate the protective role of IDPm in SH-SY5Y cells, recombinant plasmid DNA was transfected into the cells using Lipofectamine 2000, and stable transfectants for LNCX- vector alone or for LNCX-IDPm were isolated in G418-selective media. After selection, stable transfectants were screened to select clones showing the highest expression of IDPm by RT-PCR and enzyme activity assay; two clones, namely S1 and S2, were obtained. S1 and S2 cells showed marked IDPm mRNA expression whereas V cells showed very little or no IDPm transcripts (Fig. 1A). IDPm expression was also assessed by measuring isocitrate dehydrogenase enzyme activity. As shown in Figure 1B, IDPm activities were nine- and five-fold higher in S1 and S2 cells, respectively, as compared to V cells. Those S1 cells that showed the highest expressions of both mRNA and enzymatic activity were used for subsequent experiments. Mitochondrial NADPH (44.5 ± 2.2 pmol/mg) and GSH (6.8 ± 0.8 nmol/mg) levels in S1 cells were also significantly higher than those in V cells (NADPH, 27.2 ± 7.6 2 pmol/mg; GSH, 4.8 ± 0.2 nmol/mg) (Fig. 1C). However, total cellular levels of NADPH (180.0 ± 8.3 pmol/mg) and GSH (26.0 ± 0.1 nmol/mg) in S1 cells were not significantly higher than those in V cells (NADPH, 178.9 ± 6.6 pmol/mg; GSH, 26.9 ± 1.5 nmol/mg). All recombinant cells used in this study showed the same morphological phenotype and cell division rate, when compared to normal cells.

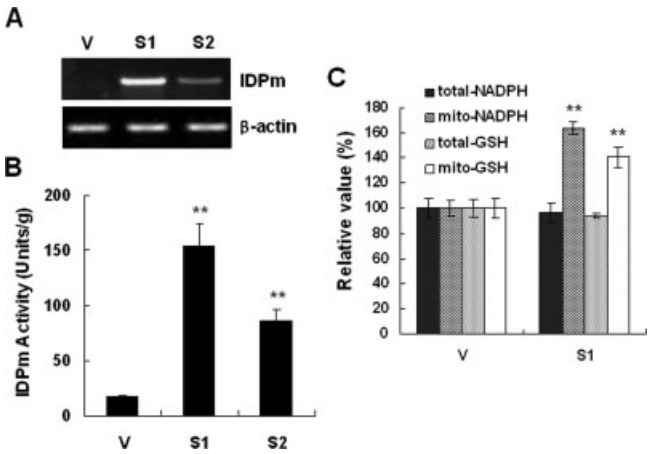

Fig. 1. Expression of IDPm in SH-SY5Y cells. SH-SY5Y cells were transfected with LNCX- vector alone (V cells), or LNCX-sense IDPm (S1, S2 cells), targeted to the mitochondria. **A:** Overexpression of IDPm was examined by RT-PCR, using specific primers for IDPm. Note that S1 and S2 recombinant cells show significant increase in IDPm mRNA expression whereas V cells showed little or no expression. β-actin was used as an internal control. **B:** Overexpression of IDPm was examined by IDPm activity assay. Mitochondrial homogenates (100 μg) were used for determining IDPm activity as described in the Materials and Methods. Note that IDPm activity was significantly higher in S1 and S2 than in V cells. Data are expressed as mean ± SD from three independent experiments. $^{**}P < 0.01$ vs. V cells. **C:** The levels of NADPH and GSH in cells (total) and mitochondria were determined in V and S1 cells. The relative percentages were obtained by referring these values to those of vector control (V, 100%). Note that the level of mitochondrial NADPH in S1 cells (44.5 ± 2.2 pmol/mg) was shown to be 1.7-fold higher than in V cells (27.2 ± 7.6 pmol/mg), whereas the total cellular level of NADPH showed no significant difference between S1 (180.0 ± 8.3 pmol/mg) and V (178.9 ± 6.6 pmol/mg) cells. Note that the level of mitochondrial GSH in S1 cells (6.8 ± 0.8 nmol/mg) was shown to be 1.4-fold higher than in V cells (4.8 ± 0.2 nmol/mg), whereas the total cellular level of GSH showed no significant difference between S1 (26.0 ± 0.1 nmol/mg) and V (26.9 ± 1.5 nmol/mg) cells. Data are expressed as a percentage relative to V cell values and represent the mean ± SD of three independent experiments. $^{**}P < 0.01$ vs. V cells.

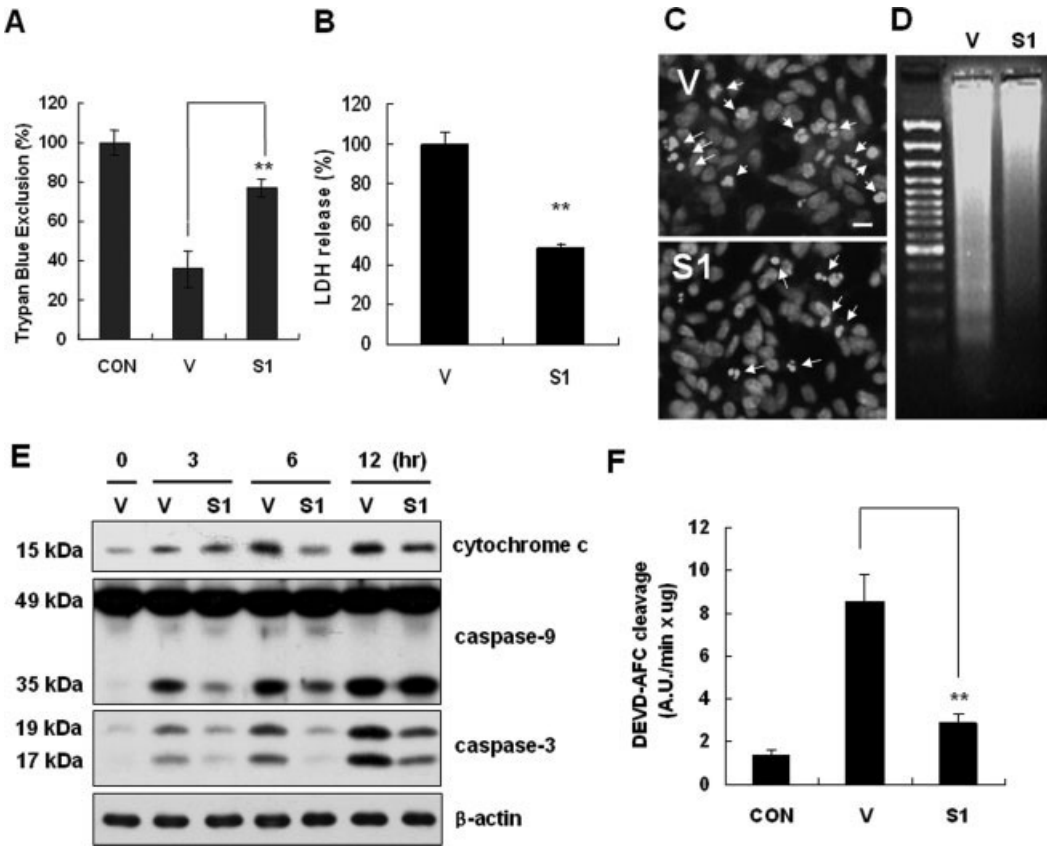

Fig. 2. Effect of overexpressed IDPm on staurosporine-induced apoptotic cell death. **A:** Cell viability was measured by the trypan blue exclusion method. Cells were seeded on 24-well plates at 1×10^5 cells per well. Twenty-four hours after staurosporine (100 nM) treatment, the numbers of cells excluding or being stained for trypan blue were counted using a hemocytometer. The percentage survival was obtained by referring these values to those of the DMSO treatment control (con). Note that survival of S1 cells was significantly higher than for V cells. $^{**}P < 0.01$ vs. V cells. **B:** Cell viability was examined by measuring LDH released into media. Cells were seeded on 24-well plates at 1×10^5 cells per well. Twenty-four hours after staurosporine (100 nM) treatment, LDH released was measured according to manufacturer's protocol. Note that survival of S1 cells was significantly higher than for V cells. The percentage of survival was obtained by referring these values to those of the LNCX-vector control. $^{**}P < 0.01$ vs. V cells. **C:** Nuclei were stained with DAPI. Cells were seeded on poly-D-lysine (50 μg/ml)-coated coverslips, and 12 hr after staurosporine treatment, DAPI-stained nuclei were observed using a fluorescent microscope equipped with CCD camera (Cool SNAP). Arrows indicate chromatin condensation and fragmentation typical of apoptosis. Note that S1 cells showed fewer apoptotic cells than did V cells. Scale bar = 10 μm. **D:** DNA laddering was detected in 2% agarose gels. Twelve hours after staurosporine treatment, DNA was obtained as described in the Materials and Methods. Note that DNA laddering was less evident in S1 cells than in V cells. The gel represents four independent experiments. **E:** Western blot analyses of cytochrome c, capase-9, and caspase-3 in V and S1 cells. At different times (0, 3, 6, and 12 hr) after staurosporine treatment, S-100 proteins were subjected to Western blot analysis as described in the Materials and Methods. Note that cytochrome c release into cytoplasm increased after staurosporine treatment, however, the release was attenuated more in S1 than in V cells. Cleavage of caspase-9 and -3 into active forms (caspase-9, 35 kDa; caspase-3, 17, 19 kDa) after staurosporine treatment was also alleviated more in S1 cells than in V cells. β-actin was used as an internal control. **F:** Caspase-3 activity was measured in V and S1 cells treated with 100 nM of staurosporine for 12 hr. Activity was quantified by monitoring the cleavage of the fluorogenic substrate DEVD-AFC (50 μM) as described in the Materials and Methods. Note that caspase-3 activation was significantly mitigated in S1 cells (2.88 ± 0.43) when compared to V cells (8.5 ± 1.3) after staurosporine treatment. Activities are represented as increases in AFC fluorescence per min per microgram of protein. Data represent mean value ± SD of three independent experiments. $^{**}P < 0.01$ vs. V cells.

Protective Role of IDPm in Staurosporine-Induced Apoptosis

It is well known that staurosporine induces apoptotic cell death in SH-SY5Y (Bertrand et al., 1994). To examine the protective role of IDPm, cells were treated with 100 nM staurosporine for 24 hr, and cell viability was examined by trypan blue exclusion assay and LDH assay. Trypan blue exclusion was significantly higher in S1 cells as compared to V cells (Fig. 2A). As shown in Figure 2B, LDH release from S1 cells was also significantly lower than from V cells. MTT assay further confirmed the protective effect of IDPm against staurosporine in S1 cells (data not shown). The specific patterns of DNA fragmentation by DAPI staining and agarose gel electrophoresis 12 hr after stauro-

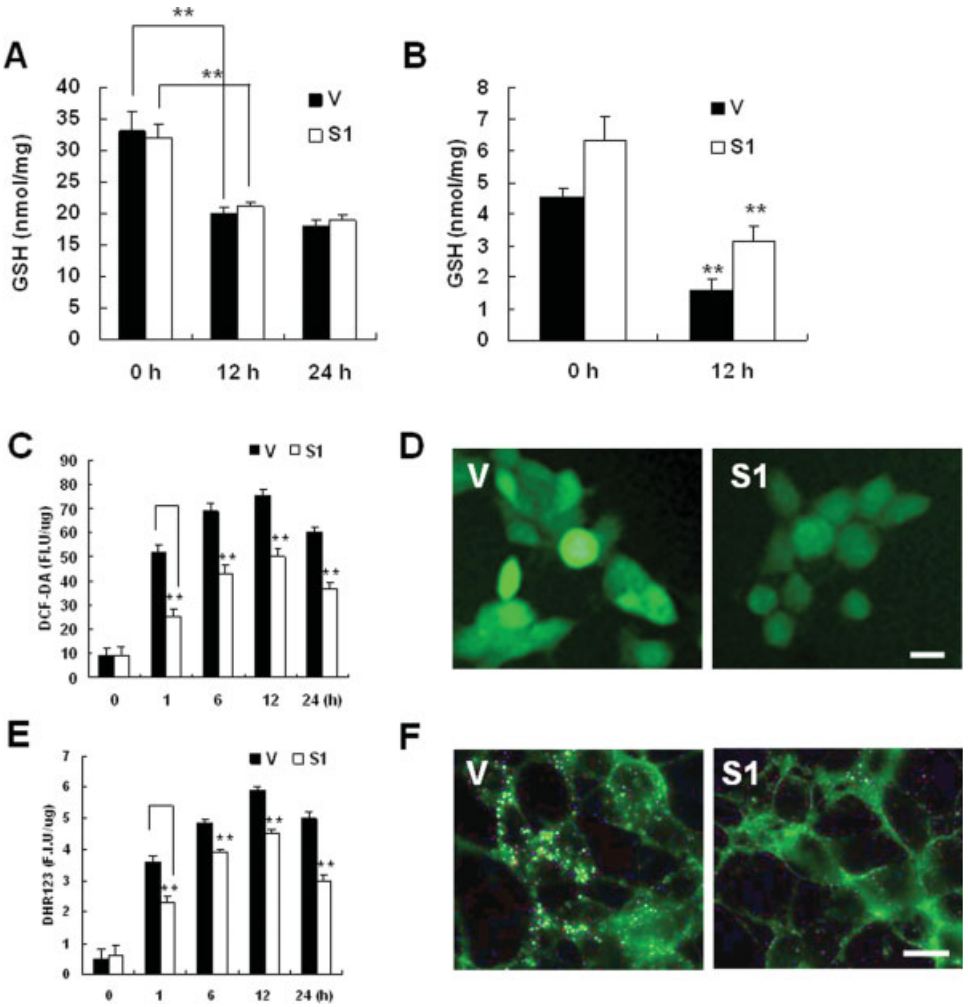

Fig. 3. Effects of overexpressed IDPm on staurosporine-induced GSH depletion and ROS production. **A:** Staurosporine treatment decreased total cellular GSH. After staurosporine treatment, cells (1×10^7) were harvested and total cell extracts were obtained as described in the Materials and Methods. Note that the levels of total cellular GSH in both V and S1 cells decreased significantly after staurosporine treatment. $^{**}P < 0.05$ vs. 0 hr. **B:** Mitochondrial GSH contents in V and S1 cells were measured after staurosporine treatment. Mitochondria (3×10^7 cells) were isolated as described in the Materials and Methods and used for GSH measurement. Note that the mitochondrial GSH levels decreased significantly in both V and S1 cells 12 hr after staurosporine treatment, however, the percent decrease was smaller in S1 cells (50%) than in V cells (65%). Data represent the mean ± SD of three independent experiments. $^{**}P < 0.05$ vs. 0 hr. **C:** Intracellular ROS was measured using DCF-DA fluorescence dye. Cells were plated on 24-well plates (1×10^5 cells per well). After staurosporine (100 nM) treatment, cells were treated with 10 μM of DCF-DA for 30 min, and oxidized dichlorofluorescein was measured using a fluorometer. The intensity of DCF-DA was expressed as an arbitrary fluorescence unit relative to μg of protein. Note that ROS levels in V cells were significantly higher than in S1 cells after staurosporine treatment. Data represent the mean ± SD of three independent experiments. $^{**}P < 0.01$ vs. V cells. **D:** Photomicrographs of DCF-DA fluorescence were taken 1 hr after staurosporine treatment using a fluorescent microscope equipped with CCD camera (Cool SNAP). Note that the intensity of DCF-DA fluorescence was higher in V than in S1 cells. Scale bar = 10 μm. **E:** Intracellular ROS was measured using DHR fluorescence dye. DHR (10 μM) was used in the same procedures as described above and expressed as an arbitrary fluorescence unit relative to μg of protein. Note that mitochondrial ROS levels in V cells were significantly higher than in S1 cells after staurosporine treatment. Data represent the mean ± SD of three independent experiments. $^{**}P < 0.01$ vs. V cells. **F:** Photomicrographs of DHR fluorescence were taken 1 hr after staurosporine treatment. Note that the intensity of DHR fluorescence in mitochondria was higher in V than in S1 cells. Scale bar = 10 μm.

sporine treatment were examined to further characterize the neuroprotective effect of IDPm. When cells were treated with staurosporine, the numbers of condensed and fragmented nuclei were fewer in S1 cells than in V cells (Fig. 2C). S1 cells also showed less DNA fragmentation than did V cells in agarose gel electrophoresis (Fig. 2D).

Effects of IDPm on Cytochrome c Release and Caspase Activation

Mitochondria-generated GSH and proteins with similar functions such as phospholipid hydroperoxide glutathione peroxidase (PHGPx) are known to inhibit oxidative stress-induced cytochrome c release from mi-

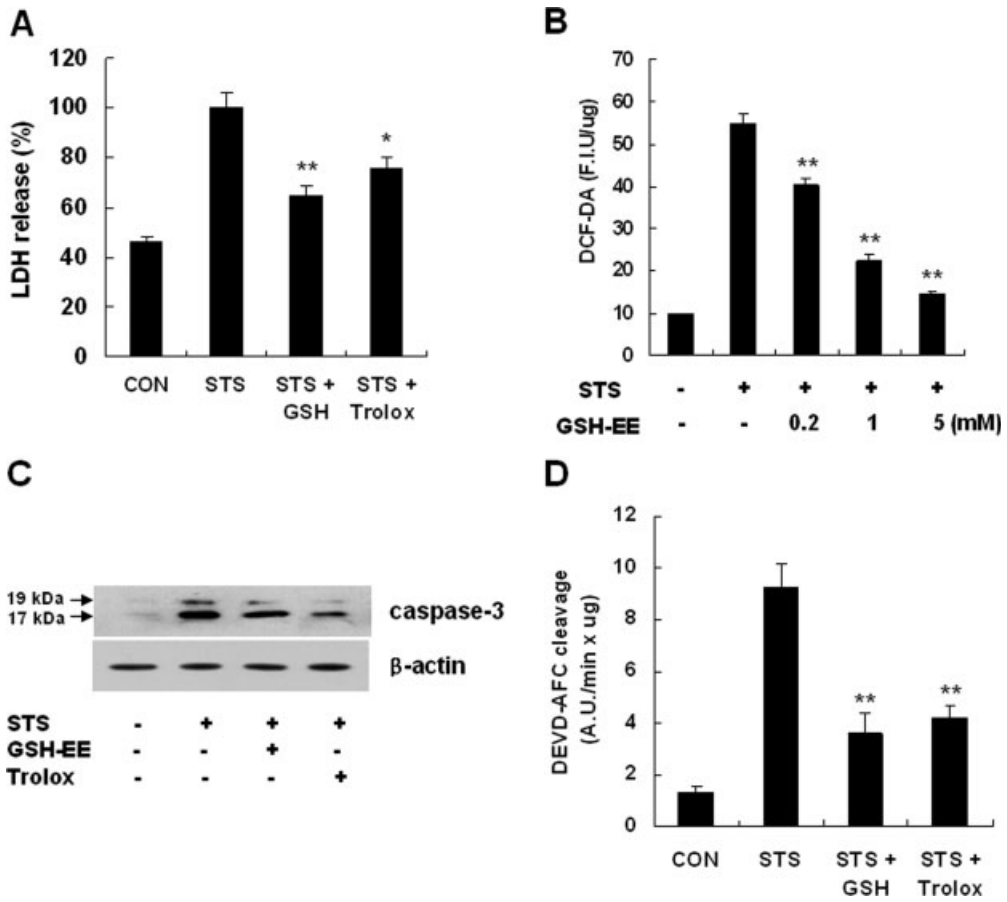

Fig. 4. Effects of antioxidants on LDH release, caspase-3 activation and ROS production after staurosporine treatment. **A:** Cells were pre-treated with trolox (1 μM) or GSH-EE (1 mM) for 1 hr. Staurosporine (100 nM) was treated for 24 hr and media were used for LDH assay. Note that GSH-EE and trolox significantly inhibited LDH release compared to staurosporine treated control. **B:** Cells were pre-treated with GSH-EE (0.2, 1, 5 mM) for 1 hr before staurosporine treatment and ROS production was measured using DCF-DA. ROS production was attenuated significantly by GSH-EE on dose dependent manner. **C,D:** Cells were pre-treated with trolox (1 μM) or GSH-EE (1 mM) for 1 hr, cellular extract after staurosporine treatment (12 hr) was subjected to Western blot and activity assay of caspase-3 using DEVD-AFC (50 μM). Note that the level of activity (**D**) and active forms (C: 17, 19 kDa) of caspase-3 was significantly attenuated by antioxidant treatment. β-actin was used as an internal control. $\star P < 0.05$, $\star\star P < 0.01$ vs. staurosporine alone.

tochondria (Nomura et al., 1999; Drake et al., 2003). The effect of overexpressing IDPm on cytochrome c release from mitochondria after staurosporine treatment was investigated because S1 cells showed an increase in mitochondrial GSH level (Fig. 1C). As shown in Figure 2E, cytochrome c release from mitochondria increased up to 12 hr after staurosporine treatment. However, cytochrome c release was markedly attenuated in S1 cells when compared to that in V cells at 3, 6, and 12 hr after staurosporine treatment. Figure 2E also showed that staurosporine treatment increased activation of caspase-9 and caspase-3. However, the active forms of caspase-9 (35 kDa) and caspase-3 (17, 19 kDa) were markedly reduced in S1 as compared to levels in V cells over the treatment intervals (Fig. 2E). Inhibition of caspase-3 activation by overexpressing IDPm was also confirmed by measuring caspase-3 activity 12 hr after staurosporine treatment. As shown in Figure 2F, caspase-3 activity was significantly reduced by more than 60% in S1 cells when compared to that in V cells.

Effect of IDPm on ROS Production and GSH Depletion After Staurosporine

Because staurosporine treatment decreases cellular glutathione redox ratio (GSH/GSH + GSSG) by reducing GSH level, (Ahlemeyer and Krieglstein, 2000; Barrachina et al., 2002), we investigated the effect of overexpressing IDPm on cellular as well as mitochondrial GSH level after staurosporine treatment. As shown in Figure 3A, the total cellular GSH level in both V and S1 cells decreased significantly after staurosporine treatment, although the total cellular NADPH level was not changed (data not shown). Although mitochondrial GSH levels also decreased in both V and S1 cells 12 hr after staurosporine treatment, the percentage decrease was

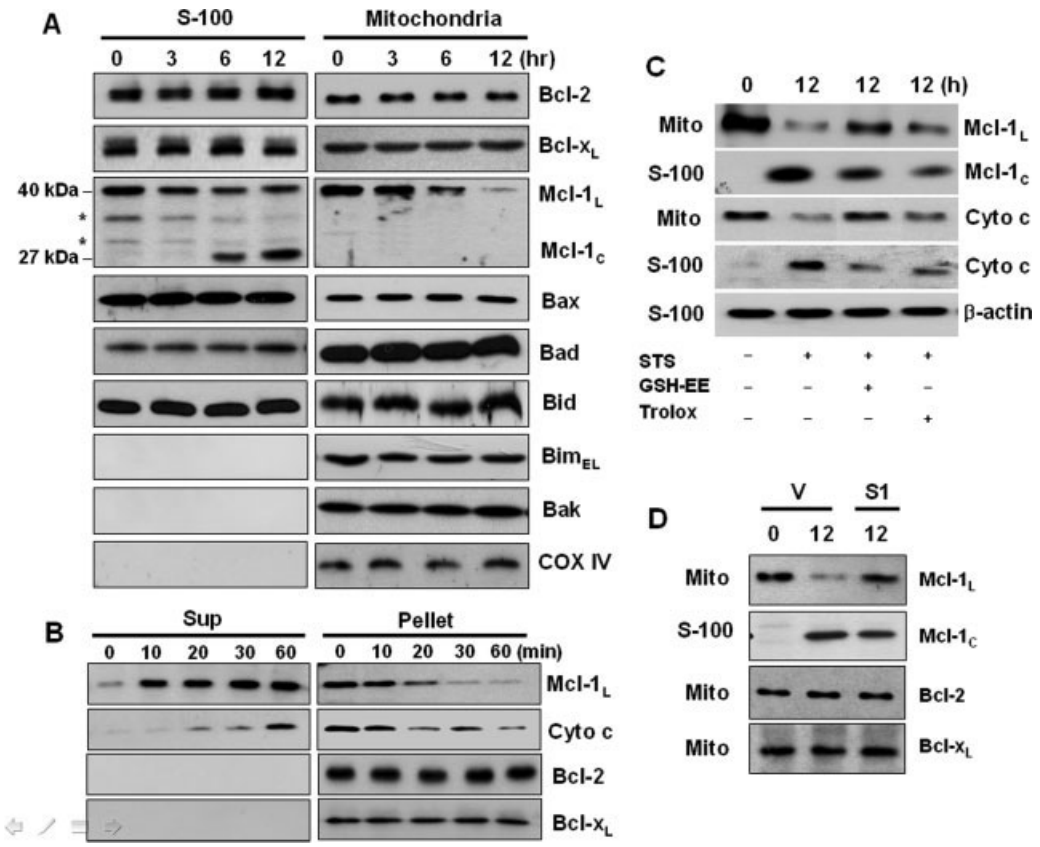

Fig. 5. Release and cleavage of Mcl-1 by staurosporine treatment. **A:** Cells were treated with staurosporine for indicated time points, S-100 (50 μg) and mitochondrial (10 μg) proteins were subjected to Western blot analyses using antibodies against anti-apoptotic proteins of the Bcl-2 family (Bcl-2, Bcl-x_L and Mcl-1) and pro-apoptotic proteins of the Bcl-2 family (Bad, Bak, Bax, Bid, and Bim_{EL}). Note that Mcl-1, as shown in both S-100 and mitochondrial fractions, was modulated after staurosporine treatment whereas other proteins of the Bcl-2 family showed no change after drug treatment. The asterisks indicate cross reactive bands. COX IV was used as a mitochondrial internal control. **B:** Mitochondria prepared from SH-SY5Y cells were incubated with staurosporine (100 nM) for indicated times (0, 10, 20, 30, and 60 min) and supernatant and pellet were subjected to Western analyses. Note that Mcl-1 were released into supernatant appeared 10 min after staurosporine treatment and followed by cytochrome c release into supernatant 20 min after treatment, whereas the levels of Mcl-1 and cytochrome c in pellet were decreased after treatment. However, the release of other proteins of the Bcl-2 family into supernatant was not observed. Sup, supernatant; Cyto c, cytochrome c. **C:** Cells were pre-treated with antioxidants, trolox (1 μM) and GSH-EE (1 mM) for 1 hr before staurosporine treatment. After 12 hr, S-100 and mitochondrial fractions were prepared and subjected to Western blot analyses. Note that Mcl-1 and cytochrome c releases from mitochondria were inhibited by GSH-EE or trolox. The cleavage product ($Mcl\text{-}1_C$, 27 kDa) of Mcl-1 in S-100 was also reduced by antioxidant treatments. **D:** S-100 (50 μg) and mitochondrial proteins (10 μg) prepared from V and S1 cells after staurosporine treatment were subjected to Western blot analyses. Note that the level of mitochondrial Mcl-1 was much lower in V cells than in S1 cells 12 hr after staurosporine treatment whereas the levels of Bcl-2 and Bcl-x_L showed no difference between V and S1 cells after drug treatment. The level of cleavage product of Mcl-1 ($Mcl\text{-}1_C$) in V cells was also higher than in S1 cells. The gel represents three independent experiments.

smaller in S1 cells (50%) than in V cells (65%) (Fig. 3B). The production of ROS after staurosporine treatment was examined using the ROS specific fluorescence dyes, DCF-DA and DHR, that are reactive mainly with cytoplasmic (Keller et al., 1998) and with mitochondrial ROS (Mattson et al., 1997), respectively. As shown in Figure 3C and E, ROS levels peaked at 12 hr in both V and S1 cells after staurosporine treatment, although both cytoplasmic and mitochondrial ROS levels were significantly lower in S1 as compared to V cells. Representative images of cells stained with DCF-DA and DHR are shown in Figure 3D and F.

Effects of Antioxidants on Cell Death, Caspase-3 Activation, and ROS Production After Staurosporine Treatment

To examine whether GSH depletion and increased ROS production after staurosporine treatment instigate cell death of SH-SY5Y, we examined the protective effects of two antioxidants, trolox, a vitamin E derivative, and GSH-ethyl ester (EE; a cell permeable form of GSH) on cell viability after staurosporine treatment. As shown in Figure 4A, LDH release was decreased significantly when cells were pre-treated with trolox (1 μM) or GSH-EE (1 mM) 1 hr before staurosporine treatment.

ROS production was also inhibited significantly when cells were pretreated with antioxidants before staurosporine treatment (Fig. 4B). Furthermore, caspase-3 activation after staurosporine treatment was attenuated by trolox or GSH-EE treatment (Fig. 4D). The inhibition of caspase-3 activity by the antioxidants was further confirmed by Western blot analysis (Fig. 4C).

Release and Cleavage of Mcl-1 by Staurosporine Treatment

It has been reported that modulation of anti-apoptotic and pro-apoptotic Bcl-2 family members are involved in cytochrome c release (Gross et al., 1999), although the exact mechanism(s) has not been elucidated. To investigate the possible mechanisms involved in cytochrome c release mediated by staurosporine-induced oxidative stress, we examined modulation in the expression of the Bcl-2 family of proteins in SH-SY5Y cells after staurosporine treatment. As shown in Figure 5A, among the proteins in the Bcl-2 family, only Mcl-1 was modulated after staurosporine treatment. Mcl-1 (Mcl-1_L, 40 kDa) levels decreased progressively in mitochondrial fractions either 3, 6, 12 hr after staurosporine treatment whereas the level of the cleaved form (Mcl-1_C, 27 kDa) increased in the S-100 fraction (Fig. 5A). By contrast, the level of other anti- and pro-apoptotic members of the Bcl-2 family were not changed in either the mitochondrial or S-100 fractions after staurosporine treatment (Fig. 5A). To investigate the release of Mcl-1 from mitochondria and its involvement in cytochrome c release, mitochondrial organelles were treated with staurosporine, and both cytochrome c and Mcl-1 release from mitochondria were examined. As shown in Figure 5B, Mcl-1_L release after staurosporine treatment from mitochondria into supernatant was evident by 10 min and followed by cytochrome c release observed at 20 min. The levels of both Mcl-1_L and cytochrome c in pellets (mitochondria) were decreased after drug treatment (Fig. 5B). However, other members of the Bcl-2 family were neither released into supernatant nor did their levels change in pellets after staurosporine treatment (Fig. 5B). When SH-SY5Y cells were pre-treated with the antioxidants, trolox (1 μM) or GSH-EE (1 mM) before staurosporine treatment, Mcl-1_L and cytochrome c levels in the mitochondrial fraction were higher than those in cells treated with staurosporine alone (Fig. 5C). By contrast, the level of the cleaved product of Mcl-1 (Mcl-1_C) in the S-100 fraction was lower in trolox- or GSH-EE-treated cells than in cells treated with staurosporine alone (Fig. 5C). Next, the effect of overexpressing IDPm on mitochondrial Mcl-1 after staurosporine treatment was examined. As shown in Figure 5D, the level of mitochondrial Mcl-1_L in S1 cells was higher than in V cells 12 hr after staurosporine treatment, whereas the level of cleavage product (Mcl-1_C) in S-100 was lower in S1 cells than in V cells (Fig. 5D).

Caspase-3 Dependent Mcl-1 Cleavage

Because Mcl-1 is known to be cleaved by caspase-3 (Weng et al., 2005), the effect of caspase-3 inhibitor on Mcl-1 cleavage was investigated to confirm whether the cleaved product of Mcl-1 appearing after staurosporine treatment was caspase-3 dependent. SH-SY5Y cells were pre-treated with zVAD-FMK, a caspase-3 inhibitor, and S-100 and mitochondrial fractions were prepared 12 hr after staurosporine treatment. As shown in Figure 6A, zVAD-FMK (1–50 μM) inhibited caspase-3 activity in a dose-dependent manner. The cleavage product of Mcl-1 (Mcl-1_C, 27 kDa) in S-100 fraction was also decreased by the caspase-3 inhibitor in a dose-dependent manner whereas no cleaved product of Mcl-1 was observed in the mitochondrial fraction (Fig. 6B). To confirm the above result, whole cell extracts were prepared from SH-SY5Y cells treated with staurosporine. The extracts prepared from SY5Y cells without staurosporine treatment were also treated with recombinant caspase-3 enzyme. The cleavage product of Mcl-1 was then examined. As shown in Figure 6C, the cleavage product of Mcl-1 (Mcl-1_C) was observed in both extracts treated with staurosporine at 6 and 12 hr and with 0.5 and 1 U of caspase-3 enzyme.

Interaction of Mcl-1 with Bim

Mcl-1 is known to complex with such pro-apoptotic proteins of the Bcl-2 family as Bim; cleavage of Mcl-1 by caspase increases its complex with Bim leading to inhibition of its anti-apoptotic function (Herrant et al., 2004). Using coimmunoprecipitation analyses, we examined if pro-apoptotic Bcl-2 molecules formed complexes with Mcl-1 in mitochondria. As shown in Figure 7A, only Bim, one of the BH-3 pro-apoptotic proteins, formed a complex with Mcl-1 in mitochondria. When S1 and V cells were treated with staurosporine, the level of mitochondrial Bim protein showed no difference between V and S1 cells (Fig. 7B). However, when V and S1 cells were treated with staurosporine, the level of the Mcl-1/Bim complex in S1 cells was higher than in V cells (Fig. 7C). Bim is known to induce loss of mitochondrial membrane potential ($\Delta\psi_m$) and cytochrome c release (Sugiyama et al., 2002). To determine the relation between the loss of $\Delta\psi_m$ and cytochrome c release, the membrane potential of mitochondria treated with staurosporine (100 nM) at the time points indicated was measured using the fluorescent dye rhodamine 123 (Rh123) that accumulates in mitochondria in a $\Delta\psi_m$-dependent manner. As shown in Figure 8A, Rh123 uptake was decreased in isolated mitochondria by staurosporine treatment, which indicates loss of $\Delta\psi_m$, whereas the DMSO-treated control showed no change in Rh123 uptake. Moreover, the loss of $\Delta\psi_m$ in intact cell was significantly attenuated in S1 cells when compared to that in V cells after staurosporine treatment (Fig. 8B).

DISCUSSION

We examined the role of mitochondrial IDPm in protection from neurotoxicity that seems to be linked to oxidative stress and to mitochondrial cytochrome c-mediated apoptosis in SH-SY5Y cells. This study first

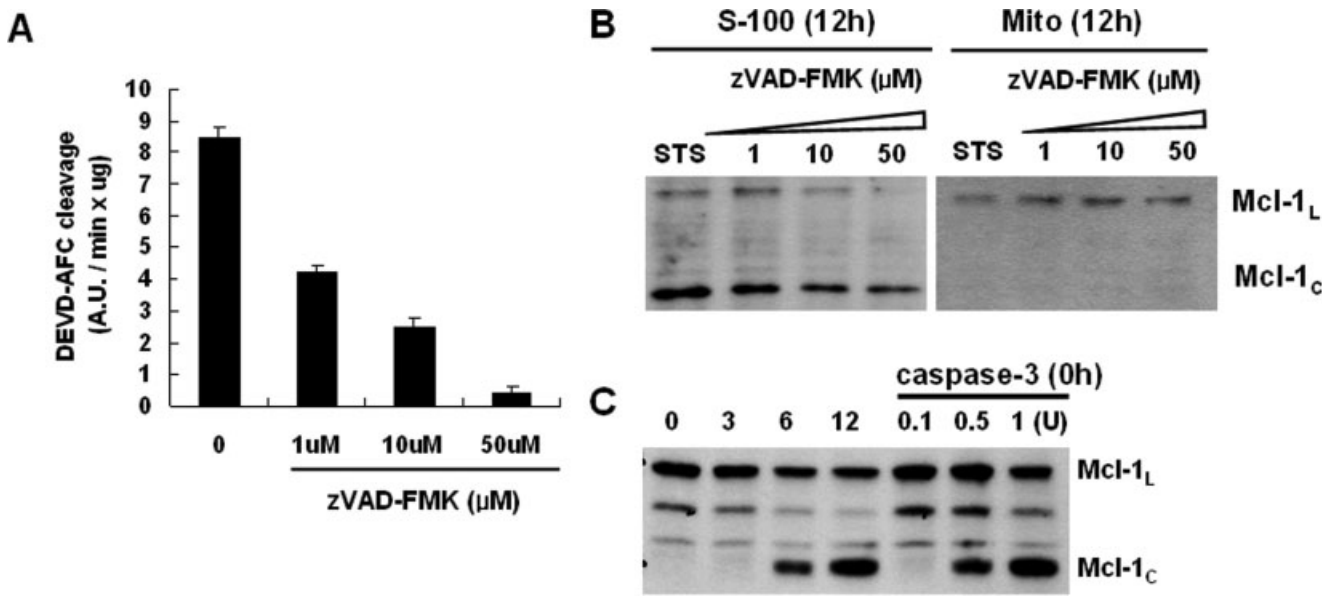

Fig. 6. Caspase-3 dependent Mcl-1 cleavage. **A:** SY5Y Cells were treated with a specific caspase-3 inhibitor, zVAD-FMK for 1 hr before staurosporine (100 nM) treatment. After 12 hr, cells were harvested and specific caspase-3 activity was measured using 50 μM of DEVD-AFC. Note that caspase-3 activity was inhibited by zVAD-FMK in a dose dependent manner. **B:** SY5Y cells were treated with 1–50 μM of zVAD-FMK for 1 hr before staurosporine treatment. After 12 hr, S-100 and mitochondrial proteins prepared as described in the Materials and Methods were subject to Western analyses. Note that the level of cleaved product of Mcl-1 (Mcl-1_C, 27 kDa) in S-100 extracts was decreased by the caspase-3 inhibitor in a dose-dependent manner, whereas no cleaved product of Mcl-1 was observed in the mitochondrial fraction. **C:** Whole cell extracts were prepared from SH-SY5Y cells treated with staurosporine as described in the Materials and Methods (lane 1–4). The extracts prepared from SY5Y cells without staurosporine treatment were also treated with recombinant caspase-3 enzyme (lane 5–7). The cleavage product of Mcl-1 in both preparations was examined by Western blot analysis. Note that the cleavage product of Mcl-1 (Mcl-1_C) was observed in the extracts treated with staurosporine and with caspase-3 enzyme. Gel represents three independent experiments.

addressed the importance of IDPm, particularly in mitochondria, to the susceptibility of neuronal cells to staurosporine-induced oxidative stress. Our data showed that S1 cells overexpressing IDPm showed more resistance to oxidative stress by attenuation of ROS production than did V cells. After staurosporine treatment, the decrease in mitochondrial GSH was smaller in S1 cells than in V cells. An exogenous supply of anti-oxidant, trolox, and GSH-EE, significantly inhibited apoptotic cell death induced by staurosporine. These observations suggest that IDPm plays a neuroprotective role by increasing the mitochondrial GSH pool, which then acts as an antioxidant against staurosporine-induced ROS. Thus, our results are in agreement with a recent report by Jo et al. (2001), which showed that in the mitochondria, IDPm, as a major producer of NADPH, is required for the regeneration of GSH and exerts a protective effect against H_2O_2-mediated oxidative stress in NIH3T3 cells. A report by Shin et al. (2004) also showed that IDPm plays an important protective role in apoptosis of HEK293 cells induced by a high concentration of glucose. It has been known that cytochrome c is released after mitochondrial damage by staurosporine and cytochrome c-mediated apoptosome formation with caspase-9 and Apaf-1 is a major operant factor in staurosporine-induced apoptosis in SH-SY5Y cells (McGinnis et al., 1999; Lopez and Ferrer, 2000).

Staurosporine is known as a broad kinase inhibitor. Staurosporine is also known to generate nitric oxide (NO) after intracellular calcium increase in PC 12 cells (Kruman et al., 1998) and mitochondrial superoxide anion after caspase-1 mediated cytochrome c release in hippocampal cultures (Krohn et al., 1998). However, several reports indicate that staurosporine treatment does not activate caspase-1 in SH-SY5Y cells (Nath et al., 1996; Bijur et al., 2000). Furthermore, as our preliminary results showed that NO was not produced during the 24 hr after staurosporine treatment (data not shown), we suggest that ROS produced by staurosporine in SH-SY5Y cells may not be mediated by caspase-1 and is unrelated to reactive nitrogen species (RNS) such as NO. In our system, ROS produced by staurosporine treatment seemed to induce the release of mitochondrial cytochrome c, as evidenced by inhibition of cytochrome c release by treatment with the antioxidants trolox or GSH-EE. Furthermore, cytochrome c release induced by staurosporine was attenuated more significantly in S1 cells overexpressing IDPm than in V cells, which suggests that IDPm inhibits cytochrome c release by increasing the level of GSH in the mitochondria. Thus,

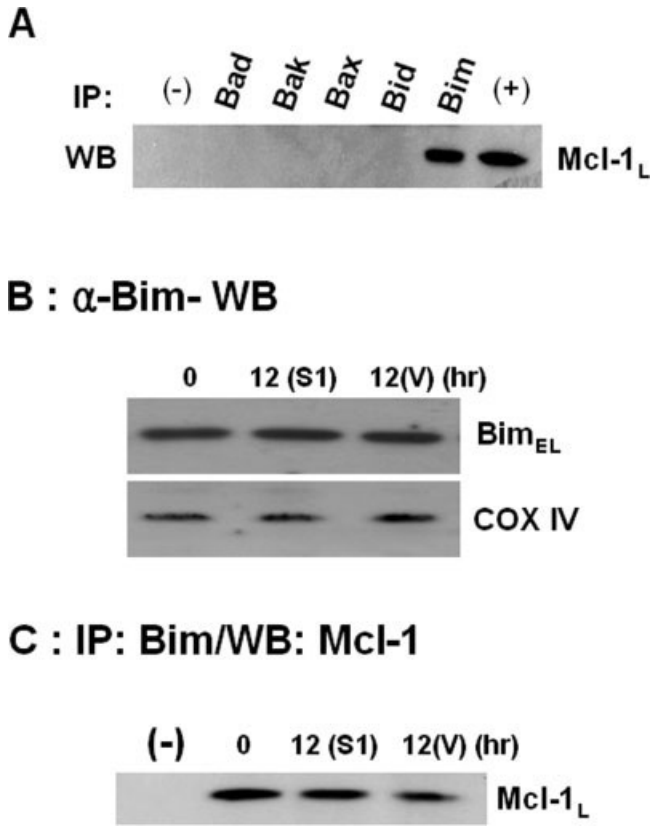

Fig. 7. Interaction of Mcl-1 with Bim. **A:** Mitochondrial proteins (300 μg) from normal cells were immunoprecipitated with antibodies against pro-apoptotic proteins of the Bcl-2 family (Bad, Bak, Bax, Bid, and Bim), and the precipitated proteins were subjected to Western blot analysis using Mcl-1 antibody. Note that only Bim formed a complex with Mcl-1 protein in mitochondria, whereas Bad, Bak, Bax, and Bid did not. The gel represents three independent experiments. IP, immunoprecipitation with antibodies against pro-apoptotic proteins of the Bcl-2 family; WB, Western blotting using Mcl-1 antibody. (−) and (+) denote IgG alone and range of cell extract, respectively. **B:** Mitochondrial proteins (10 μg) from V and S1 cells after staurosporine treatment for 12 hr were subjected to Western blot using Bim antibody. Note that the level of mitochondrial Bim protein showed no difference in V and S1 cells. WB, Western blotting using Bim antibody. **C:** Mitochondrial proteins (300 μg) from the V and S1 cells 12 hr after staurosporine treatment were immunoprecipitated with Bim antibody, and the precipitated proteins were subjected to Western blot analysis with Mcl-1 antibody. Note that the level of Mcl-1/Bim complex was higher in S1 cells than in V cells. The gel represents three independent experiments. IP, immunoprecipitation with Bim antibody; WB, Western blotting using Mcl-1 antibody.

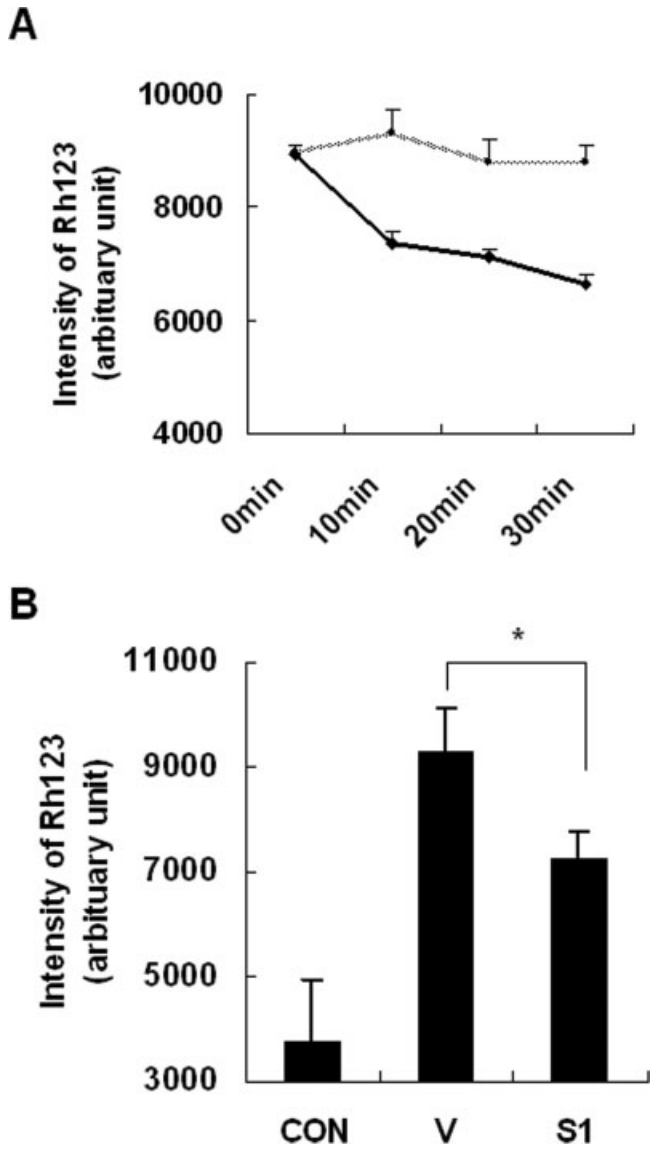

Fig. 8. The attenuation of the loss of mitochondrial membrane potential ($\Delta\psi_m$) in S1 cells. **A:** Mitochondria isolated from SH-SY5Y cells were treated with staurosporine (100 nM). Mitochondrial membrane potential ($\Delta\psi_m$) was measured based on the rhodamine 123 (Rh123, 50 nM) uptake over 30 min at room temperature. Note that Rh123 uptake by the mitochondria was decreased after staurosporine treatment. Dashed line: control (0.1% DMSO), solid line: staurosporine. **B:** Cells were pre-equilibrated with Rh123 (10 μM) and washed three times with Locke's solution. Then cells were treated with staurosporine (100 nM) and the fluorescence was measured 10 min after staurosporine treatment. Note that more Rh123 was retained significantly in S1 cells when compared to that in V cells after staurosporine treatment. Data represent mean ± SD of three independent experiments. $^{\star}P < 0.05$ vs. V cells.

our results are consistent with the fact that mitochondrial GSH is known to inhibit oxidative stress-induced cytochrome c release from mitochondria (Drake et al., 2003).

In vivo, GSH is produced by the liver, transported in the blood and can cross the blood-brain barrier (Kannan et al., 1992). A cell line model could be more susceptible to lack of GSH whereas this limitation may not affect the mitochondrial pool of GSH. However, the effect of GSH depletion on neuronal viability has been widely studied in several experimental models of neurodegenerative diseases in vivo and in vitro. For example, GSH depletion is the first indicator of oxida-

tive stress during PD; the magnitude of GSH depletion seems to parallel the severity of the disease and occurs before other hallmarks of the disease including decreased activity of mitochondrial complex I (Sian et al., 1994; Jha et al., 2000). Also, the depletion of mitochondrial GSH by ethacrynic acid (EA) treatment in the CNS produces higher level of ROS leading to cell death, whereas depletion of the cytosolic GSH pool due to buthionine sulfoximine (BSO) treatment does not (Seyfried et al., 1999; Roychowdhury et al., 2003). Thus, it seems that the depletion of mitochondrial GSH increases oxidative stress in pathologic conditions and in some case induces further ROS accumulation leading to cell death. Our study also showed that staurosporine treatment induced apoptotic cell death in SH-SY5Y cells and increased ROS production, which was significantly attenuated by overexpressing IDPm or by pretreatment with the antioxidants, trolox, or GSH-EE before drug treatment, thereby inhibiting apoptotic cell death. Therefore, these results indicate that staurosporine-induced toxicity was mediated by GSH depletion followed by ROS production in mitochondria, leading to apoptotic cell death. Furthermore, GSH produced in association with IDPm activity can be considered as an important therapeutic target molecule for the various neurologic disorders mediated by GSH depletion after oxidative stress.

Previous reports have shown that the balance between the pro- and anti-apoptotic members of the Bcl-2 family determines the mitochondrial response to apoptotic stimuli (Adams and Cory, 2001). Anti-apoptotic proteins such as Bcl-2, Bcl-x_L, and Mcl-1 protect mitochondrial integrity, whereas the pro-apoptotic members of the family promote the release of apoptogenic proteins such as cytochrome c from the mitochondria. It has also been suggested that Bcl-2 can modulate sensitivity to oxidative stress through the regulation of GSH content (Gendron et al., 2001) although the exact mechanism(s) of its action is not known. However, our results showed that only Mcl-1 was modulated after staurosporine treatment, whereas other anti-apoptotic proteins of the Bcl-2 family such as Bcl-2 and Bcl-x_L were not changed in SH-SY5Y cells. Mcl-1 was released from the mitochondria by staurosporine treatment, which was attenuated by exogenous antioxidants such as trolox and GSH-EE. Furthermore, staurosporine treatment induced cytochrome c release from mitochondria followed by the release of Mcl-1. These observations thus suggest that Mcl-1 is released by staurosporine-induced ROS and that Mcl-1 release from mitochondria may be involved in the release of mitochondrial cytochrome c into cytoplasm after staurosporine treatment.

Mcl-1 is an anti-apoptotic member of the Bcl-2 protein family, a critical regulator of apoptosis in normal and malignant cells (Michels et al., 2005). Mcl-1 has also been known to have a short half-life, and to be regulated post-translationally by phosphorylation (Inoshita et al., 2002; Michels et al., 2005) and ubiquitination after proteasome-mediated degradation (Nijhawan et al., 2003; Zhong et al., 2005). Nijhawan et al. (2003) reported that the elimination of cytosolic inhibitors such as Mcl-1 and Bcl-x_L is required for the release of mitochondrial cytochrome c and subsequent caspase activation. Our results showed that when mitochondrial organelles were treated with staurosporine, Mcl-1 was gradually released from mitochondria, whereas the level of Mcl-1 in supernatant increased. However, other members of the Bcl-2 family were not released from mitochondria by staurosporine treatment. Furthermore, the phosphorylation and degradation of Mcl-1 did not likely occur because the total amount of cellular Mcl-1 did not seem to be changed 12 hr after staurosporine treatment. It has been reported that Mcl-1 can complex with the pro-apoptotic members of the Bcl-2 family of proteins such as Bim, Bak, and t-Bid (Herrant et al., 2004; Weng et al., 2005; Willis et al., 2005). Cleavage of Mcl-1 by caspase modifies its subcellular localization and increases its association with Bim, leading to inhibition of its anti-apoptotic function (Herrant et al., 2004). Our study showed that Mcl-1 released from mitochondria by staurosporine treatment was cleaved to a shortened form in a caspase-3 dependent manner, and its release was attenuated far more in S1 than in V cells after staurosporine treatment. Cleavage of Mcl-1 by caspase-3 yields two specific fragments with molecular masses of 27 and 19 kDa by tumor necrosis factor-related apoptosis-inducing ligand, which becomes pro-apoptotic in Jurkat cells (Herrant et al., 2004). Only the Mcl-1 cleavage product of 27 kDa produced by caspase-3 was observed in this study. Whether it is pro-apoptotic is yet to be determined. Furthermore, intact Mcl-1 formed a complex with Bim in mitochondria and the level of the complex in S1 was higher than in V cells after staurosporine treatment.

Release of cytochrome c from mitochondria is considered to be a key initial step in the apoptotic process. Although the manner of release and precise mechanisms regulating cytochrome c release remain unknown, it has been suggested that cytochrome c release is mediated by the mitochondrial outer membrane permeabilization through the action of proapoptotic factors such as Bax/Bak pore opening (Korsmeyer et al., 2000; Pagliari et al., 2005), the oligomerization of the VDAC (Zalk et al., 2005), or through the dissipation of the membrane potential through VDAC/ANT interaction (Sade et al., 2004). Bim is also known to induce loss of mitochondrial membrane potential ($\Delta\psi_m$) and cytochrome c release (Sugiyama et al., 2002). We showed that Rh123 uptake was decreased by staurosporine treatment, which indicates loss of $\Delta\psi_m$. In considering the decrease of the $\Delta\psi_m$ and the attenuation of the loss of $\Delta\psi_m$ in S1 cells as compared to that of V cells after staurosporine treatment (Fig. 8), our data suggest that the release of Mcl-1 by staurosporine may result in an increase in the pool of free Bim molecules, which might be involved in the loss of the mitochondrial $\Delta\psi_m$, leading to cytochrome c release from mitochondria. The direct evidence for involvement of Bim in the loss of $\Delta\psi_m$ and the interaction with the VDAC was not determined and will have to await future studies. These observations lead us to

hypothesize that Mcl-1 release may facilitate the pro-apoptotic activity of Bim, leading to cytochrome c release from mitochondria and the anti-apoptotic activity of IDPm may result from maintaining the Mcl-1/Bim complex, thereby inhibiting Mcl-1 release from mitochondria after staurosporine treatment.

In mammalian mitochondria, there are two classes of isocitrate dehydrogenase (ICDH), NAD^+-dependent ICDH (IDH) and $NADP^+$-dependent ICDH (IDPm). IDH is known to participate in the oxidative decarboxylation of isocitrate in the citric acid cycle (Cupp and McAlister-Henn, 1991) and IDPm activity is modulated through enzymatic glutathionylation and deglutathionylation during oxidative stress (Kil and Park, 2005). The function of IDPm in the nervous system is not known. IDPm is highly expressed in heart, skeletal muscle, and liver but exists in relatively low levels in brain (Jo et al., 2001). Such tissue specific expression may explain why each tissue such as brain and heart may have a different susceptibility to oxidative stress. Although the role of IDPm in the nervous system has not yet been elucidated, brain may be more susceptible to oxidative stress followed by GSH depletion. Moreover, GSH depletion in PD, aging, and ischemic injury have been correlated with the severity of symptoms (Sofic et al., 1992; Bains and Shaw, 1997; Anderson and Sims, 2002). The IDPm-mediated production of mitochondrial NADPH may be particularly important in neural tissues that are more highly susceptible to oxidative stress. Nevertheless, the present study is the first to show a protective role for IDPm in neuronal cells. Our results also suggest that the preservation of the intact mitochondria and redox status, through supplementation of GSH via IDPm, might protect neuronal cells against mitochondrial damage mediated by oxidative stress. The protein IDPm may provide a therapeutic site of opportunity for preventing neuronal cell death occurring in neurodegenerative diseases and after injury.

ACKNOWLEDGMENTS

LNCX and LNCX-IDPm constructs were gifts from Dr. T.L. Huh, Dept. of Genetic Engineering, College of Natural Sciences, Kyungpook National University, Korea.

REFERENCES

Adams JM, Cory S. 2001. Life-or-death decisions by the Bcl-2 protein family. Trends Biochem Sci 26:61–66.

Ahlemeyer B, Krieglstein J. 2000. Inhibition of glutathione depletion by retinoic acid and tocopherol protects cultured neurons from staurosporine-induced oxidative stress and apoptosis. Neurochem Int 36:1–5.

Anderson MF, Sims NR. 2002. The effects of focal ischemia and reperfusion on the glutathione content of mitochondria from rat brain subregions. J Neurochem 81:541–549

Bains JS, Shaw CA. 1997. Neurodegenerative disorders in humans: the role of glutathione in oxidative stress-mediated neuronal death. Brain Res Rev 25:335–358.

Barrachina M, Secades J, Lozano R, Gomez-Santos C, Ambrosio S, Ferrer I. 2002. Citicoline increases glutathione redox ratio and reduces caspase-3 activation and cell death in staurosporine-treated SH-SY5Y human neuroblastoma cells. Brain Res 957:84–90.

Bertrand R, Solary E, O'Connor P, Kohn KW, Pommier Y. 1994. Induction of a common pathway of apoptosis by staurosporine. Exp Cell Res 211:314–321.

Bhamre S, Nuzzo RL, Whitin JC, Olshen RA, Cohen HJ. 2000. Intracellular reduction of selenite into glutathione peroxidase. Evidence for involvement of NADPH and not glutathione as the reductant. Mol Cell Biochem 211:9–17.

Bijur GN, De Sarno P, Jope RS. 2000 Glycogen synthase kinase-3beta facilitates staurosporine- and heat shock-induced apoptosis. Protection by lithium. J Biol Chem 275:7583–7590.

Canals S, Casarejos MJ, de Bernardo S, Rodriguez-Martin E, Mena MA. 2003. Nitric oxide triggers the toxicity due to glutathione depletion in midbrain cultures through 12-lipoxygenase. J Biol Chem 278:21542–21549.

Cupp JR, McAlister-Henn L. 1991. NAD(+)-dependent isocitrate dehydrogenase. Cloning, nucleotide sequence, and disruption of the IDH2 gene from Saccharomyces cerevisiae. J Biol Chem 266:22199–22205.

Deneke SM, Fanburg EL. 1989. Regulation of cellular glutathione. Am J Physiol 257:L163–L173.

Drake J, Sultana R, Aksenova M, Calabrese V, Butterfield DA. 2003. Elevation of mitochondrial glutathione by γ-glutamylcysteine ethyl ester protects mitochondria against peroxynitrite-induced oxidative stress. J Neurosci Res 74:917–927.

Ehrenberg B, Montana V, Wei MD, Wuskell JP, Loew LM. 1988. Membrane potential can be determined in individual cells from the nernstian distribution of cationic dyes. Biophys J 53:785–794.

Esworthy RS, Ho YS, Chu FF. 1997. Gpx1 gene encodes mitochondrial glutathione peroxidase in the mouse liver. Arch Biochem Biophys 340:59–63.

Gabby M, Tauber M, Porat S, Simantov R. 1996. Selective role of glutathione in protecting human neuronal cells from dopamine-induced apoptosis. Neuropharmacology 35:571–578.

Gaetani GF, Galiano S, Canepa L, Ferraris AM, Kirkman HN. 1989. Catalase and glutathione peroxidase are equally active in detoxification of hydrogen peroxide in human erythrocytes. Blood 73:334–339.

Gendron MC, Schrantz N, Metivier D, Kroemer G, Maciorowska Z, Sureau F, Koester S, Petit PX. 2001. Oxidation of pyridine nucleotides during Fas- and ceramide-induced apoptosis in Jurkat cells: correlation with changes in mitochondria, glutathione depletion, intracellular acidification and caspase-3 activation. Biochem J 353:357–367.

Griffith OW, Meister A. 1985. Origin and turnover of mitochondrial glutathione. Proc Natl Acad Sci U S A 82:4668–4672.

Gross A, McDonnell JM, Korsmeyer SJ. 1999. BCL-2 family members and the mitochondria in apoptosis. Genes Dev 13:1899–1911.

Herrant M, Jacquel A, Marchetti S, Belhacene N, Colosetti P, Luciano F, Auberger P. 2004. Cleavage of Mcl-1 by caspases impaired its ability to counteract Bim-induced apoptosis. Oncogene 23:7863–7873.

Hsu M, Srinivas B, Kumar J, Subramanian R.Anderson J. 2005. Glutathione depletion resulting in selective mitochondrial complex I inhibition in dopaminergic cells is via an NO-mediated pathway not involving peroxynitrite: implications for Parkinson's disease. J Neurochem 92:1091–1103.

Inoshita S, Takeda K, Hatai T, Terada Y, Sano M, Hata J, Umezawa A, Ichijo H. 2002. Phosphorylation and inactivation of myeloid cell leukemia 1 by JNK in response to oxidative stress. J Biol Chem 277:43730–43734.

Inoue M. 1989. Glutathione: dynamic aspect of protein mixed disulfide formation. In: Dorphin D, Avramovie O, Poulsen R, editors. Glutathione chemical biological and medical aspects. Part B. New York: Wiley. p 613–641.

Jha N, Jurma O, Lalli G, Liu Y, Pettus EH, Greenamyre JT, Liu RM, Forman HJ, Anderson JK. 2000. Glutathione depletion in PC12 results in selective inhibition of mitochondrial complex I activity. Implications for Parkinson's disease. J Biol Chem 275:26096–26101.

Jo SH, Son MK, Koh HJ, Lee SM, Song IH, Kim YO, Lee YS, Jeong KS, Kim WB, Park JW, Song BJ, Huh TL. 2001. Control of mitochondrial redox balance and cellular defense against oxidative damage by mitochondrial NADP+-dependent isocitrate dehydrogenase. J Biol Chem 276:16168–16176.

Kannan R, Kuhlenkamp JF, Ookhtens M, Kaplowitz N. 1992. Transport of glutathione at blood-brain barrier of the rat: inhibition by glutathione analogs and age-dependence. J Pharmacol Exp Ther 263:964–970.

Keller JN, Guo Q, Holtsberg FW, Bruce-Keller AJ, Mattson MP. 1998. Increased sensitivity to mitochondrial toxin-induced apoptosis in neural cells expressing mutant presenilin-1 is linked to perturbed calcium homeostasis and enhanced oxyradical production. J Neurosci 18:4439–4450.

Kil IS, Park JW. 2005. Regulation of mitochondrial NADP+-dependent isocitrate dehydrogenase activity by glutathionylation. J Biol Chem 280:10846–10854.

Korsmeyer SJ, Wei MC, Saito M, Weiler S, Oh KJ, Schlesinger PH. 2000. Pro-apoptotic cascade activates BID, which oligomerizes BAK or BAX into pores that result in the release of cytochrome c. Cell Death Differ 7:1166–1173.

Krohn AJ, Preis E, Prehn JH. 1998. Staurosporine-induced apoptosis of cultured rat hippocampal neurons involves caspase-1-like proteases as upstream initiators and increased production of superoxide as a main downstream effector. J Neurosci 18:8186–8197.

Kruman I, Guo Q, Mattson MP. 1998. Calcium and reactive oxygen species mediate staurosporine-induced mitochondrial dysfunction and apoptosis in PC12 cells. J Neurosci Res 51:293–308.

Lee SM, Yune TY, Kim SJ, Kim YC, Oh YJ, Markelonis GJ, Oh TH. 2004. Minocycline inhibits apoptotic cell death via attenuation of TNF-α expression following iNOS/NO induction by lipopolysaccharide in neuron/glia co-cultures. J Neurochem, 91:568–578.

Lopez E, Ferrer I. 2000. Staurosporine- and H-7-induced cell death in SH-SY5Y neuroblastoma cells is associated with caspase-2 and caspase-3 activation, but not with activation of the FAS/FAS-L-caspase-8 signaling pathway. Brain Res Mol Brain Res 85:61–67.

Mattson MP, Goodman Y, Luo H, Fu W, Furukawa K. 1997. Activation of NF-κB protects hippocampal neurons against oxidative stress-induced apoptosis: evidence for induction of Mn-SOD and suppression of peroxynitrite production and protein tyrosine nitration. J Neurosci Res 49:681–697.

McGinnis KM, Gnegy ME, Wang KK. 1999. Endogenous bax translocation in SH-SY5Y human neuroblastoma cells and cerebellar granule neurons undergoing apoptosis. J Neurochem 72:1899–1906.

Michels J, Johnson PW, Packham G. 2005. Mcl-1. Int J Biochem Cell Biol 37:267–271.

Nath R, Raser KJ, Stafford D, Hajimohammadreza I, Posner A, Allen H, Talanian RV, Yuen P, Gilbertsen RB, Wang KK. 1996. Non-erythroid alpha-spectrin breakdown by calpain and interleukin 1 beta-converting-enzyme-like protease(s) in apoptotic cells: contributory roles of both protease families in neuronal apoptosis. Biochem J 319:683–690.

Nijhawan D, Fang M, Traer E, Zhong Q, Gao W, Du F, Wang X. 2003. Elimination of Mcl-1 is required for the initiation of apoptosis following ultraviolet irradiation. Genes Dev 17:1475–1486.

Nomura K, Imai H, Koumura T, Arai M, Nakagawa Y. 1999. Mitochondrial phospholipid hydroperoxide glutathione peroxidase suppresses apoptosis mediated by a mitochondrial death pathway. J Biol Chem 274:29294–29302.

Pagliari LJ, Kuwana T, Bonzon C, Newmeyer DD, Tu S, Beere HM, Green DR. 2005. The multidomain proapoptotic molecules Bax and Bak are directly activated by heat. Proc Natl Acad Sci U S A 102:17975–18980.

Plaut GWE, Gabriel JL. 1983. Biochemistry of metabolic process. New York: Elsevier Science Publishing Co. p 285–301.

Roychowdhury S, Wolf G, Keilhoff G, Horn TF. 2003. Cytosolic and mitochondrial glutathione in microglial cells are affected differentially affected by oxidative/nitrosative stress. Nitric Oxide 8:39–47.

Sade H, Khandre NS, Mathew MK, Sarin A. 2004. The mitochondrial phase of the glucocorticoid-induced apoptotic response in thymocytes comprises sequential activation of adenine nucleotide transporter (ANT)-independent and ANT-dependent events. Eur J Immunol 34:119–125.

Schulz JB, Lindenau J, Seyfried J, Dichgans J. 2000. Cytosolic and mitochondrial glutathione in microglial cells are affected differentially affected by oxidative/nitrosative stress. Eur J Biochem 267:4904–4911.

Seyfried J, Soldner F, Schulz JB, Klockgether T, Kovar KA, Wullner U. 1999. Differential effects of L-buthionine sulfoximine and ethacrynic acid on glutathione levels and mitochondrial function in PC12 cells. Neurosci Lett 264:1–4.

Shin AH, Kil IS, Yang ES, Huh TL, Yang CH, Park JW. 2004. Regulation of high glucose-induced apoptosis by mitochondrial NADP+-dependent isocitrate dehydrogenase. Biochem Biophys Res Commun 325:32–38.

Sian J, Dexter DT, Lees AJ, Daniel S, Agid Y, Javoy-Agid F, Jenner P, Marsden CD. 1994. Alterations in glutathione levels in Parkinson's disease and other neurodegenerative disorders affecting basal ganglia. Ann Neurol 36:348–355.

Sofic E, Lange KW, Jellinger K, Riederer P. 1992. Reduced and oxidized glutathione in the substantia nigra of patients with Parkinson's disease. Neurosci Lett 142:128–130.

Spina MB, Squinto SP, Miller J, Lindsay RM, Hyman C 1992. Brain-derived neurotrophic factor protects dopamine neurons against 6-hydroxydopamine and N-methyl-4-phenylpyridinium ion toxicity: involvement of the glutathione system. J Neurochem 59:99–106.

Sugiyama T, Shimizu S, Matsuoka Y, Yoneda Y, Tsujimoto Y. 2002. Activation of mitochondrial voltage-dependent anion channel by a pro-apoptotic BH3-only protein Bim. Oncogene 21:4944–4956.

Tay VK, Wang AS, Leow KY, Ong MM, Wong KP, Boelsterli UA. 2005. Mitochondrial permeability transition as a source of superoxide anion induced by the nitro aromatic drug nimesulide in vitro. Free Radic Biol Med 39:949–959.

Wagner TC, Scott MD. 1994. Single extraction method for the spectrophotometric quantitation of oxidized and reduced pyridine nucleotides in erythrocytes. Anal Biochem 222:417–426.

Weng C, Li Y, Xu D, Shi Y, Tang H. 2005. Specific cleavage of Mcl-1 by caspase-3 in tumor necrosis factor-related apoptosis-inducing ligand (TRAIL)-induced apoptosis in Jurkat leukemia T cells. J Biol Chem 280:10491–14500.

Willis SN, Chen L, Dewson G, Wei A, Naik E, Fletcher JI, Adams JM, Huang DC. 2005. Proapoptotic Bak is sequestered by Mcl-1 and Bcl-xL, but not Bcl-2, until displaced by BH3-only proteins. Genes Dev 19:1294–1305.

Woltjer RL, Nghiem W, Maezawa I, Milatovic D, Vaisar T, Montine KS, Montine TJ. 2005. Role of glutathione in intracellular amyloid-alpha precursor protein/carboxy-terminal fragment aggregation and associated cytotoxicity. J Neurochem 93:1047–1056.

Zalk R, Israelson A, Garty ES, Azoulay-Zohar H, Shoshan-Barmatz V. 2005. Oligomeric states of the voltage-dependent anion channel and cytochrome c release from mitochondria. Biochem J 386:73–83.

Zhong Q, Gao W, Du F, Wang X. 2005. Mule/ARF-BP1, a BH3-only E3 ubiquitin ligase, catalyzes the polyubiquitination of Mcl-1 and regulates apoptosis. Cell 121:1085–1095.